International Journal of Enhanced Research in Science Technology & Engineering, ISSN: 2319-7463
Vol. 4 Issue 6, June-2015, pp: (86-98), Impact Factor: 1.252, Available online at: www.erpublications.com

Optical Constants of KDPTGS Single Crystals

A. Abu El-Fadl[1*], A. M. Nashaat[2]
[1,2]Physics Department, Faculty of Science, Assiut University, 71516 Assiut, Egypt

Abstract: Single crystals of KDP doped TGS crystals (KDPTGS) were synthesized and grown by slow evaporation solution growth technique. KDPTGS easily crystallizes in monoclinic system with space group $P2_1/c$. Using the transmittance and reflectance spectra, the optical energy gap and optical constants have been determined. Peculiar changes in the optical constants of single crystals of triglycine sulfate (TGS) pure and doped with different concentrations of potassium dihydrogen phosphate. It was found that, the absorption coefficient (α), indirect optical band gap ($E_g^{opt.}$), refractive index (n) and the extinction coefficient (k) decreased with increasing dopant concentration. The refractive index dispersion data were analyzed using the Wemple-Di Domenico single-effective-oscillator model. As a result, the oscillator energy, dispersion energy, oscillator strength, and zero-frequency refractive index were determined. The values obtained for the single-oscillator energy E_{so} are nearly consistent with the optical gap results. The dependence of the optical constants of KDPTGS on the photon energy (ħω) at different concentrations of KDP were discussed.

Keywords: KDPTGS crystals, Optical energy gap, Normal dispersion, Optical constants.

1- Introduction

Crystals of triglycine sulfate abbreviated as (TGS) is a well-known ferroelectric material, find wide application as room temperature IR detectors [1, 2]. TGS is one of the very few ferroelectrics known to exhibit a second-order phase transition and hence offers possibilities for the observation of genuinecritical phenomenon very close to the Curie temperature. TGS is anorder-disordertype ferroelectrics with a transition from ferroelectric to paraelectric phase at 322 K, having high pyroelectric coefficient and low dielectric constant values [3].

Ferroelectric properties of TGS crystals have been found to change strongly under the action of different kinds of admixtures [4,5]. Many authors have investigated the effect of various doping on TGS [6-11]. Single crystals of triglycine sulfate (TGS) doped with various L-form amino acids (L-valine, L-leucine, and L-isoleucine) have been prepared by Nakatani et al. [12]. Doping effects on the crystal morphology and the ferroelectric domain structure, and the generation of internal bias field were investigated. For crystals grown from solutions with L-valine, L-leucine, and L-isoleucine, both the morphology and the domain structures were resemble to pure TGS. Many studies have been performed with different metallic ion dopants such as Cu^{2+}, Li^{+}, Mn^{2+}, Ni^{2+}, Cr^{3+},which have been added to modify the properties of TGS crystals[13-16]. Rare earth metal ions admixture TGS crystals, such as La, Ce and Nd modified the morphology and coercive field values[13].

The interest in studying pure and doped TGS crystals has increased because of their promise in various devices. Several dopants have been recently used, more or less successful, to inhibit the ferroelectric switching of TGS, in order to increase crystal unipolarity and the figure of merit of material[14].The influence of the KDP doping on the pyroelectric and the dielectric properties of the TGS crystal was studied by Sooman Leeet al. [17]. Their results confirmed that, with increasing KDP doping, the coercive field increased and the Curie temperature decreased. Moreover, improved pyroelectric properties were observed.

The optical constants define how light interacts with a material. The determination of these optical constants is expected to expand the available physical information about the spectral dependence of optical parameters such as refractive index, dielectric constant, reflectivity and absorption coefficients are essential in characterizing materials that are used in the fabrication of optoelectronic devices[18].

The investigations on TGS doped with ferroelectric and antiferroelectric crystals are not studied in details. In the present work, the influence of KDP dopant concentration on the TGS crystal optical parameters has been studied. The dispersion of the refractive index is discussed in terms of the Wemple-DiDomenico single-effective-oscillator model. The refractive

index dispersion parameters: oscillator energy, dispersion energy, oscillator strength, and zero-frequency refractive index were estimated.

2-Experimental Procedures

Single crystals of TGS $(NH_2CH_2COOH)_3$ H_2SO_4 doped with different concentrations of potassium dihydrogen phosphate KH_2PO_4 (KDP) were grown by the slow evaporation method in the ferroelectric phase at about 315 K. The concentrations of KDP were 10%, 20%, 30%, 40%and 50% relative to H_2SO_4. The calculated amount of material was dissolved in double distilled water at room temperature and the reactants were thoroughly dissolved and stirred well for about 6 hour using a temperature controlled magnetic stirrer to obtain a homogeneous mixture of solution. The solution was allowed to evaporate at room temperature, which yielded colorless crystalline salt of KDPTGS. The purity of the synthesized compound was further improved by successive recrystallization process. The saturated solution (about 400 ml) was prepared at room temperature based on solubility data by using water as a solvent. To eliminate difference in growth condition from our discussions, crystals with different KDP concentrations were grown simultaneously in a multi-jar crystallizer.

After preliminary experiments, optimum growth parameters including solution purity, seed, orientation and purity, seed rotational speed, starting temperature of crystallization and period of growing crystal were chosen for best result. After 2~3 weeks a single nucleation started and seed crystals with were harvested. Good optical quality seed crystals free from defects and inclusions are used for the growth of crystals from its saturated solution using suspended seed technique. After a span of about 30 days flawless crystals of optical quality and with well-developed faces were obtained sizes upto 25×15×4 mm^3. The normal external shape (habit) of doped crystals is modified due to unequal growth rate along the ferroelectric axis in opposite directions. The crystals are transparent and their shape and size is sensitive to the amount of KDP in the solution during growth. With increasing concentration of KDP in solution, the size of the crystals increases up to a molar concentration of 20–30% of KDP and decreases at a higher concentration. More details about the grown crystals are shown elsewhere [19]. The amount of KDP (mol%) incorporated into the crystal is very low. It was reported that, a factor of 10^{-2} in comparison to the actual amount taken in the solution obtained for the amount of H_3PO_4 present in the solution of TGSP crystals [20].

The crystals were cleaved parallel to (010) plane and then reduced to the required thickness. In most cases, this thickness was in the order of 1 mm..Cleaved rectangular b-cut plates about 20 mm^2 in area and 1 mm in thickness specimens were prepared and then polished on a wet piece of soft cloth to be used for optical measurements. The samples used for measurements were clear, transparent and free from any noticeable defects. Specimens prepared with these dimensions to fit the sample holder, and the sample was fixed to the holder by special glue. The optical transmission spectra measured in the photon energy range 190-900 nm at room temperature were determined using Shimadzu UV-VIS-2101 PC dual beam scanning spectrophotometer. The incident unpolarized light was nearly perpendicular to b-plane. The surrounding medium was air. For the same samples, the optical reflectance was recorded by using the same spectrophotometer in the same wavelength range. The reflectance measurements were made using specular reflectance attachment at an incidence angle of 5°, where the sample should be placed horizontally on the stage facing downward and was illuminated from the bottom. Reflectance measurements were performed, also, at room temperature.

3-Results and discussion

3.1. Optical transition

The transmittance T(λ) and reflectance R(λ) spectra are shown in **Fig. 1**. By using those spectrums, the optical energy gap and optical constants have been determined. **Fig. 1-a** shows the spectral distribution of transmittance in the spectral range 200–800 nm. The transmittance spectra of TGSK crystals decrease with increasing KDP ratio. Transmittance (T) gradually rises towards longer wavelength until it reaches its maximum value at about 350 nm. At shorter wavelengths, transmittance decreases rather quickly, and approaches near zero at around 230 nm. It is obvious that transmission edge is slightly affected by the KDP doping. It is also observed that the intensity of transmittance within the absorption region decreases by increasing KDP ratio. The reflectance spectra (**Fig. 1-b**) of the crystals show some peaks lies in the wavelength range of 200-500 nm, then show a slight decrease with the increase in wavelength up to 800 nm.

The absorption spectra of KDPTGS single crystals have been investigated at photon energies near the fundamental absorption region, and the absorption coefficient (α) obeys the equation [21]:

$$\alpha\hbar\omega \propto (\alpha\hbar\omega - E_g^{opt.})^m \qquad (1)$$

where, ħω is the energy of incident photon, $E_g^{opt.}$ is the optical energy gap and mis an exponent which can be assumed to have values of 1/2, 3/2, 2 and 3, depending on the nature of electronic transition responsible for absorption. Parameter mequals 1/2 for allowed direct transition, m=3/2 represents forbidden direct transition, m=2 for allowed indirect transition and m=3 for forbidden indirect transition. To determine the type of optical transition, we have examined $(\alpha\hbar\omega)^2$, $(\alpha\hbar\omega)^{2/3}$, $(\alpha\hbar\omega)^{1/3}(\alpha\hbar\omega)^{1/2}$versusħω and found that the last relation yielded a linear dependence, which describes allowed indirect transitions. The energy gap is determined by plotting $(\alpha\hbar\omega)^{1/2}$ as a function ofħωas depicted in **Fig. 2**andtaking the extrapolation of the linear portion of the curve to α=0.The indirect energy gap value was found to be as shown in the inset of **Fig. 2**, and listed in**Table.1**. The presented data reveals that, the increase of KDP concentration leads to an increase of the band gap $E_g^{opt.}$ and saturates at 30 mol% of KDP doping, which is nearly similar with data presented in literature [22]. Their single crystal and powder XRD studies confirmed that a certain amount of HNO_3 is doped into TGS and that there is saturation in the doping level already at 20 mol% HNO_3 addition. Further increase in HNO_3 content in solution acted as additive and enabled the changes only in crystal habit.

3.2. Normal dispersion and its parameters

3.2.1. Refractive index and extinction coefficient

The complex refractive index is a representation of the optical constants of material and is represented by ñ = n + ik. The real part 'n' is the index of refraction, defines the phase velocity of light in material: v = c/n, where v is the speed of light in material and c is the speed of light in vacuum. The imaginary part 'k' is the extinction coefficient, determines how fast the amplitude of the wave decreases. The extinction coefficient is directly related to the absorption of material and is related to the absorption coefficient by: α = 4πk/λ, where, α is the absorption coefficient and λ is the wavelength of light. The reflectance (R) in terms of the absorption coefficient and refractive index (n) can be derived from the relations [23]:

$$n = \left(\frac{1+\sqrt{R}}{1-\sqrt{R}}\right) \qquad (2)$$

The extinction coefficient (k) can be calculated using the equation:

$$k = \frac{\alpha\lambda}{4\pi} \qquad (3)$$

The frequency dispersion of$\tilde{\varepsilon}$characterizes completely thepropagation, reflection and loss of light in material.This provides us with information about the electronic structure of the material. Therefore,$\tilde{\varepsilon}$is an important quantity for the design ofhighly efficient optoelectronic devices[24].The complex dielectric constant is described by:

$$\tilde{\varepsilon} = \varepsilon_r - \varepsilon_i \text{Andtan}\,\delta = \frac{\varepsilon_i}{\varepsilon_r} \qquad (4)$$

The real $\boldsymbol{\varepsilon_r}$ and imaginary $\boldsymbol{\varepsilon_i}$ parts of the dielectric constant are related to n and k by the relations:

$$\varepsilon_r = n^2 - k^2 \qquad (5)$$

$$\varepsilon_i = 2nk \qquad (6)$$

The variation of refraction index (n), extinction coefficient (k), real (ε_r) and imaginary (ε_i) parts of the dielectric constant as a function of wavelength λ for TGS crystal doped with different concentrations of KDP ratio is shown in **Figs. 3&4**. **Fig. 3-a**shows the obtained spectral variation of the refractive index n in the wavelength range 200–800 nm, for TGS crystals doped with different KDP ratios. KDPTGS crystals showed similar behavior of n vs. λ and the values differ with KDP ratio. It also shows anomalous dispersion at wavelengths λ<450 nm exhibiting various peaks. At wavelengths λ>450 nm, in the non-absorbing region, the variation shows normal dispersion. An absorption band is observed in the wavelength range 250-280 nm and other two absorption bands in the wavelength ranges330–360 and 400–500nm. The amplitude of these bands decreases upon increasing KDP ratio. Further, the refractive index decreases with increasing the KDP ratio; this may be due to doping TGS with KDP which could change the density and/or the polarization of the grown crystal. From **Fig. 3-b**, we can see that the extinction coefficient k reverse the behavior of the transmittance. It is clear from **Fig. 4** that the variation of ε_r follows the same trend as that of n, whereas the variation of ε_i mainly follows the behavior of k which is related to the variation of α with photon energy. The real dielectric constant shows values larger than that for imaginary dielectric constant at the studied photon energy. The variation of the dielectric constant with photon energy indicates that different

interactions between photons and electrons in KDPTGS crystals a reproduced in this energy range. These interactions are observed on the shapes and cause formation of peaks in the dielectric spectra which depends on the material type. The real and imaginary parts of the dielectric constant ε_r and ε_i can be also used to calculate the spectral behavior of the optical conductivity according to the following relations [25]:

$$\sigma^* = \sigma_r + \sigma_i \qquad (7)$$

$$\sigma_r = \omega\,\varepsilon_o\varepsilon_2 \text{and} \quad \sigma_i = \omega\,\varepsilon_o\varepsilon_1 \qquad (8)$$

Where ω is the angular frequency, ε_o is the permittivity of free space. The spectra of real and imaginary parts of the optical conductivity are shown in **Fig.5**. It can be seen that both the real and imaginary part increases with increasing the photon energy up to 2.6 eV which can be attributed to excitation of electrons by photon energy. Real part of optical conductivity continues increasing sharply beyond 5.2 eV of photon energy as seen in **Fig. 5** suggesting strong excitation of the electrons. The optical conductivities σ_r and σ_i can be used to detect any further interband transitions. From the obtained data in **Fig.5**, it is noted that there are one distinct peaks for both σ_r and σ_i for different KDP ratios. The origin of this one peak in each ratio may be attributed to the optical interband transition. The increased of optical conductivity at high photon energies is due to the high absorbance of KDPTGS crystals and may be due to electron excited by photon energy.

For further analysis of the experimental results, the electric susceptibility χ_c can be calculated according to the relation [26]:

$$\varepsilon_r = \varepsilon_o + 4\pi\chi_c = n^2 - k^2 \qquad (9)$$

$$\chi_c = \frac{(n^2 - k^2 - \varepsilon_o)}{4\pi} \qquad (10)$$

Where, ε_o is the dielectric constant in the absence of any contribution from free carriers. The values of electric susceptibility χ_c for KDPTGS crystals were plotted in **Fig. 6**and the calculated values at 5eV are listed in **Table.**1.

3.2.2. Wemple–DiDomenico dispersion relation

The data of the spectral dependence of the refractive index in the transparent region, at low optical frequencies could be analyzed in terms of a single oscillator model, following the parameterization suggested by Wemple and DiDomenico [27, 28]. The dispersive refractive index data in $\hbar\omega < E_g^{opt.}$ range were analyzed according to the single-effective-oscillator model proposed by Wemple and DiDomenico. The refractive index isrelated to photon energy through the relationship:

$$n^2 = 1 + \frac{E_{so}E_d}{E_{so}^2 - (\hbar\omega)^2} \qquad (11)$$

Where, E_{so} is the single oscillator energy and E_d is the dispersion energy. Values of the parameters (E_{so} and E_d) can be evaluated by plotting of $(n^2-1)^{-1}$ versus $(\hbar\omega)^2$ and fitting it to a straight line as shown in **Fig.7**. From the fitting the found values are given in **Table. 1**.

The moments of optical dispersion spectra M_{-1}, andM_{-3}, can be evaluated using the relationships [25]:

$$E_{so}^2 = \frac{M_{-1}}{M_{-3}} \qquad (12)$$

$$E_d^2 = \frac{M_{-1}^3}{M_{-3}} \qquad (13)$$

The zero-frequency refractive index (static refractive index) is obtained using eq. (11),by putting ħω = 0, i.e. based on the expression:

$$n_o^2 - 1 = \frac{E_d}{E_{so}} \qquad (14)$$

Furthermore the values of static refractive index (zero-frequency refractive index)n_0 are also calculated and recorded in **Table. 1**. In terms of n_0 , one can see its decreasing with increasing KDP concentration which means that the static dielectric constant $\varepsilon_{sta.}$ (dielectric constant at ħω = 0) will be smaller after doping TGS crystal with KDP. This can be explained by rewriting eq. (14) as:$\varepsilon_{sta.} = n_0^2$. The values are shown in **Tables. 1, 2.**

The values of dispersion parameters and the optical moments of KDP doped TGS gathered in **Table. 1**.,arestrongly agree with Wemple [27] and Di Domentic [28]. It is clear from the table that both values of single oscillator energy (E_{so})and dispersion energy (E_d)decrease. Decreasing the single oscillator energy E_{so} (decreasing the oscillator natural frequency ω_0) with increasing KDP concentration means that the normal dispersion region of TGS crystal shifts to a range of lower photon energies by doping it with KDP. On the other hand, decreasing the dispersion energy E_d with increasing KDP concentration means that the intensity of the interband optical transitions of TGS crystal decreases by doping it with KDP. In addition, doping TGS crystal with KDP leads to decreasing its dispersion (dn/dE) due to the increase of the slope [$d(n^2-1)^{-1}/d(\hbar\omega)^2$] with increasing KDP concentration as it is clear in **Fig. 7**.

Table. 1. Normal dispersion of pure TGS and KDP doped TGS single crystals.

KDP ratio (mol%)	$E_g^{opt.}$(eV)	E_{so}(eV)	E_d (eV)	$M_{-1}(eV)^2$	M_{-3} $(eV)^{-2}$	χ_c	n_0
0 (pure)	4.912	5.006	6.604	1.319	0.053	0.315	1.523
10	4.915	4.946	5.683	1.149	0.047	0.258	1.466
20	4.928	6.337	8.08	1.275	0.032	0.212	1.508
30	4.963	6.061	5.922	0.977	0.027	0.202	1.406
40	4.966	5.157	3.919	0.76	0.029	0.185	1.327
50	4.969	4.121	1.965	0.477	0.028	0.173	1.215

The refractive index n can also be analyzed to determine the oscillator strength S_{so} for KDPTGS crystals. The refractive index is represented by a single Sellmeier oscillator at low energies [29]:

$$\frac{n_o^2-1}{n^2-1} = 1 - (\frac{\lambda_{so}}{\lambda})^2 \qquad (15)$$

Where λ_{so} is the oscillator wavelength. If we put $S_{so} = (n_o^2 - 1)/\lambda_{so}^2$. We can rewrite Eq. (15) as:

$$\frac{1}{(n^2-1)} = \frac{1}{\lambda_{so}^2 S_{so}} - \frac{1}{\lambda^2 S_{so}} \qquad (16)$$

$S_{so}$is the average oscillator strength. The plotting of $(n^2-1)^{-1}$versus λ^{-2} shows linear part edge as shown in **Fig.8**.The intersection with $(n^2-1)^{-1}$axis is $1/\lambda_{so}^2 S_{so}$ and the slope is $1/S_{so}$. Hence, the values of S_{so}andλ_{so}were determined andlisted in **Table. 2**.

3.2.3 Lattice dielectric constant ε_L and contribution of charge carrier (N)

The obtained data of refractive index n, can be analyzed to obtain the lattice dielectric constant ε_L.The relation between optical real part of dielectric constant ε_r and the square of wavelength λ^2 is given by [30]:

$$\varepsilon_r = n^2 - k^2 = \varepsilon_L - \frac{e^2}{4\pi^2 c^2 \varepsilon_o}\frac{N}{m^*}\lambda^2 \qquad (17)$$

Where e is the electronic charge, ε_L is infinite high frequency dielectric constant, $\varepsilon_o$the permittivity of free space ($8.854\times10^{-12}\ F/m$), c is the velocity of light, and N/m^* is the ratio of carrier concentration to the effective mass. The lattice dielectric constant ε_L can be obtained from plotting n^2as a function of λ^2as shown in **Fig.9**. Extrapolating the linear part of this dependence to zero wavelength give value of ε_L and from the slope the values of N/m^* were calculated. The obtained values of ε_L and N/m^* are given in the **Table. 2**. It can be noticed that the N/m^*ratio decreases with increasing KDP concentration. In general, N/m^*ratio is related to the internal microstructure. Most of the

changes in the N/m^*ratio are corresponding to the change in the carrier concentration N. Such behavior may be interpreted as that increasing KDP ratio creates additional trapping carriers which unite with the original carrier in the grown crystal.

Table. 2. Optical parameters of pure TGS and KDP doped TGS single crystals.

KDP ratio (mol%)	$N/m^* (m^3.kg)^{-1}$	λ_{so} (nm)	$S_{so}(nm)^{-2}$	ε_L	$\varepsilon_{sta.}$
0 (pure)	2.959 x 10^{57}	261.083	1.871 x 10^{-5}	3.361	2.319
10	2.668x 10^{57}	258.998	1.678 x 10^{-5}	3.087	2.149
20	1.408 x 10^{57}	202.164	3.085 x 10^{-5}	2.797	2.275
30	1.214 x 10^{57}	211.969	2.147 x 10^{-5}	2.425	1.977
40	1.476 x 10^{57}	240.757	1.312 x 10^{-5}	2.294	1.76
50	2.137 x 10^{57}	302.992	0.513 x 10^{-5}	2.191	1.477

Conclusions

From the absorbance and reflectance spectra for KDPTGS crystals, we observed that the absorption bands shift towards the smaller wavelength with the increase of KDP concentration, and the value of transmission and reflection decreases with the increases of KDP ratio**.** The indirect optical energy gap for the grown crystalsdecreases with the increase of dopant concentration**.** Optical transmission and reflectance spectrums are used to calculate the optical, electric and dielectric properties (i.e. the refractive index, extinction coefficient, optical and electrical conductivity), for KDPTGS crystals. extinction coefficient k, refractive index n and the (realε_r, imaginaryε_i) parts of dielectric constant decrease with the increase of KDP concentration for KDPTGS crystals. The wavelength dispersion behavior of grown crystals has been revealed that the average single oscillator energy for electronic transitions (E_{so}) and dispersion energy or oscillator strength (E_d) of optical transitions and their values are found to be strongly dependent on the KDP ratio.The values obtained for the single-oscillator energy E_{so} arenearly consistent with the optical gap results.The optical conductivity increased with increasing photon energy. The optical transparency of KDPTGScrystals increased over the entire recorded UV-VIS-NIR spectrum. The enhanced optical transparency and band-gap envisage the suitability of the grown crystals for SHG applications.

References

[1]. Günter Hofmann, Norbert Neumann,Helmut Budzier, Pyroelectric single-element detectors and arrays based on modified TGS**,** Ferroelectrics 133 (1992) 41– 45.DOI:http://dx.doi.org/10.1080/00150199208217975
[2]. S. Satapathy, S.K. Sharma, A.K. Karnal, V.K. Wadhawan, Effect of seed orientation on the growth of TGS crystals with large (0 1 0) facets needed for detector applications, J. Cryst. Growth 240 (2002) 196–202. DOI: http://dx.doi.org/10.1016/S0022-0248(01)02135-2
[3]. P. J. Lock, Doped Triglycine Sulfate for Pyroelectric Applications, Appl. Phys. Lett. 19 (1971) 390. DOI: http://dx.doi.org/10.1063/1.1653742
[4]. M. Gaffar, G. Al-Noaimi, A. Abu El-Fadl, Critical Behaviour of Dielectric Permittivity and Spontaneous Polarization of TriglycineSulphate Single Crystals Doped with Organic Molecules, J. Phys. Society of Japan 58 (1989) 3392–3400. DOI: http://dx.doi.org/10.1143/JPSJ.58.3392
[5]. J. Eisner, The physical properties of TGS single crystals, grown from aqueous TGS solutions containing aniline, Ferroelectrics 17 (1977) 575–578. DOI: http://dx.doi.org/10.1080/00150197808236781
[6]. G. Arunmozhi, S. Lanceros-Méndez, E. de Matos Gomes, Antiferroelectric ADP doping in ferroelectric TGS crystals, Mater. Lett. 54 (2002) 329–336. DOI: http://dx.doi.org/10.1016/S0167-577X(01)00588-2
[7]. K. Meera, R. Muralidharan, A.K. Tripathi, P. Ramasamy, Growth and characterisation of l-threonine, dl-threonine and l-methionine admixtured TGS crystals, J. Cryst. Growth 263 (2004) 524–531. DOI: http://dx.doi.org/10.1016/j.jcrysgro.2003.11.058
[8]. R.Muralidharan, R.Mohankumar, R.Dhanasekaran, A.K.Tirupathi, R.Jayavel, P.Ramasamy,Investigations on the electrical and mechanical properties of triglycinesulphate single crystals modified with some rare earth metal ions, Mater. Lett. 57 (2003) 3291–3295. DOI: http://dx.doi.org/10.1016/S0167-577X(03)00050-8

[9]. L. Prokopova, J. Novotny, Z. Micka, V. Malina, Growth of TriglycineSulphate Single Crystals Doped by Cobalt (II) Phosphate, Cryst. Res. Technol. 36 (2001) 1189–1195. DOI: http://dx.doi.org/10.1002/1521-4079(200111)36:11<1189::AID-CRAT1189>3.0.CO;2-3
[10]. J Novotný, L Prokopová, Z Mička, TGS single crystals doped by Pd(II) ions, J. Cryst. Growth 226 (2001) 333–340. DOI: http://dx.doi.org/10.1016/S0022-0248(01)01278-7
[11]. M.A. Gaffar, A. Abu El-Fadl, Effect of Doping and Irradiation on Optical Parameters of TriglycineSulphate Single Crystals, Cryst. Res. Technol. 34 (1999) 915–923. DOI: http://dx.doi.org/10.1002/(SICI)1521-4079(199908)34:7<915::AID-CRAT915>3.0.CO;2-W
[12]. N. Nakatani, T. Kikuta, T. Yamazaki, Growth and Domain Structure of TGS Crystals Doped with Various Amino Acids, Ferroelectrics 368 (2008) 12–22. DOI: http://dx.doi.org/10.1080/00150190802367380
[13]. R. Muralidharan, R. Mohankumar, P.M. Ushasree, R. Jayavel, P. Ramasamy, Effect of rare-earth dopants on the growth and properties of triglycinesulphate single crystals, J. Cryst. Growth 234 (2002) 545–550. DOI: http://dx.doi.org/10.1016/S0022-0248(01)01723-7
[14]. C.S. Fang, Yao Xi, A.S. Bhalla, L.E. Cross, Growth and properties of manganese and lithium doped TGS crystals, Mater. Res. Bull. 18 (1983) 1095–1100. DOI:http://dx.doi.org/10.1016/0025-5408(83)90152-6
[15]. A. Abu El-Fadl , Optical properties of TGS crystals doped with metal ions in the vicinity of phase transition, Physica B269 (1999) 60–68. DOI:http://dx.doi.org/10.1016/S0921-4526(99)00054-X
[16]. A. Abu El-Fadl, Effect of divalent-ions-doping on the absorption spectra and optical parameters of triglycinesulphate crystals, J. Phys. Chem. Solids 60 (1999) 1881–1893. DOI:http://dx.doi.org/10.1016/S0022-3697(99)00147-X
[17]. Sooman Lee, Kyewan Lee, Gwangseo Park, Influence of KDP doping on the pyroelectric properties of ferroelectric triglycine sulfate, J. Korean Phys.Soc 30 (1997) 261–264. DOI: http://dx.doi.org/10.3938/jkps.30.261
[18]. T. S. Moss, G. J. Burrel, E. Ellis, Semiconductor Opto-electronics, Butterworths, London (1973).
[19]. A. Abu El-Fadl, A.M. Nashaat, Crystal Growth and Physical Properties of KDP Admixtured TGS Single Crystals, Archives of Physics Research 5 (2014) 19–28.
[20]. A. Saxena, V. Gupta, K. Sreenivas, Characterization of phosphoric acid doped TGS single crystals, J. Cryst. Growth 263 (2004) 192–202. DOI: http://dx.doi.org/10.1016/j.jcrysgro.2003.10.083
[21]. M.Banan, A.K.Batra, R.B.Lal, Growth and morphology of triglycinesulphate (TGS) crystals, J. Mater. Sci. Lett. 8 (1989) 1348–1349. DOI: http://dx.doi.org/10.1007/BF00721517
[22]. R. Parimaladevi, C. Sekar, V. Krishnakumar, The effect of nitric acid (HNO_3) on growth, spectral, thermal and dielectric properties of triglycinesulphate (TGS) crystal, Spectrochim. Acta, Part A 75 (2010) 617–623. DOI:http://dx.doi.org/10.1016/j.saa.2009.11.027
[23]. H. Hasegawa, S. Yazaki, T. Shimizu, Effects of annealing on gap states in amorphous Si films, Solid State Commun. 26 (1978) 407–410. DOI: http://dx.doi.org/10.1016/0038-1098(78)90515-X
[24]. U. Zhokhavets, R. Goldhahn, G. Gobsch, W. Schliefke, Dielectric function and one-dimensional description of the absorption of poly(3-octylthiophene), Synth. Met. 138 (2003) 491–495. DOI: http://dx.doi.org/10.1016/S0379-6779(02)00502-7
[25]. Y. Caglara, S. Ilican, M. Caglar, Single-oscillator model and determination of optical constants of spray pyrolyzed amorphous SnO_2 thin films, Eur. Phys. J. B 58 (2007) 251–256. DOI: http://dx.doi.org/10.1140/epjb/e2007-00227-y
[26]. V. Gupta, A. Mansingh, Influence of post deposition annealing on the structural and optical properties of sputtered zinc oxide film, J. Appl. Phys. 80 (1996) 1063–1073. DOI: http://dx.doi.org/10.1063/1.362842
[27]. S. H. Wemple, M. DiDomenico, Jr., Behavior of the Electronic Dielectric Constant in Covalent and Ionic Materials, Phys. Rev. B 3 (1971) 1338–1351. DOI: http://dx.doi.org/10.1103/PhysRevB.3.1338
[28]. S.H. Wemple, M. DiDomenico, Optical Dispersion and the Structure of Solids, Phys. Rev. Lett. 23 (1969) 1156–1159. DOI: http://dx.doi.org/10.1103/PhysRevLett.23.1156
[29]. A. K. Walton, T. S. Moss, Determination of Refractive Index and Correction to Effective Electron Mass in PbTe and PbSe, Proc. Phys. Soc. 81(1963) 509–513.DOI:http://dx.doi.org/10.1088/0370-1328/81/3/319
[30]. P.O. Edward, Hand Book of Optical Constants of Solids, Academic Press, New York, 1985.

Figures Used

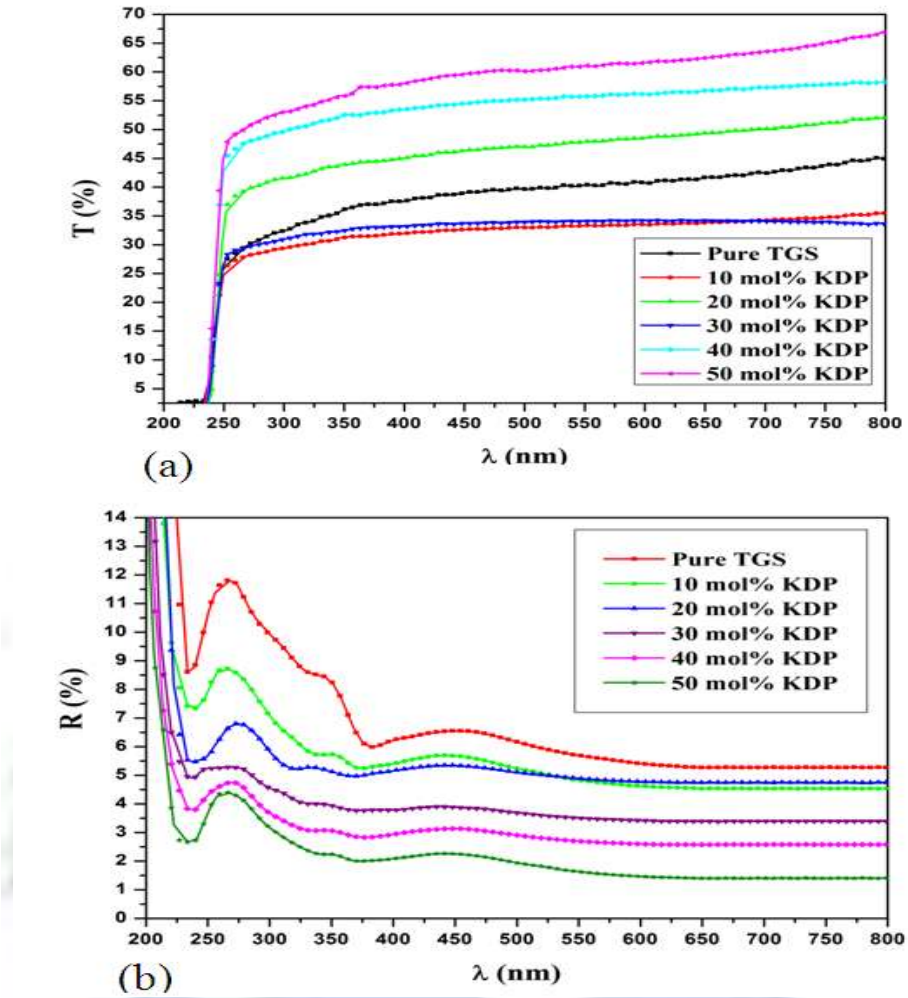

Fig. 1. Spectral distribution of normal incidence of (a) Transmittance T (λ) and (b) Reflectance R(λ) for KDPTGS single crystals.

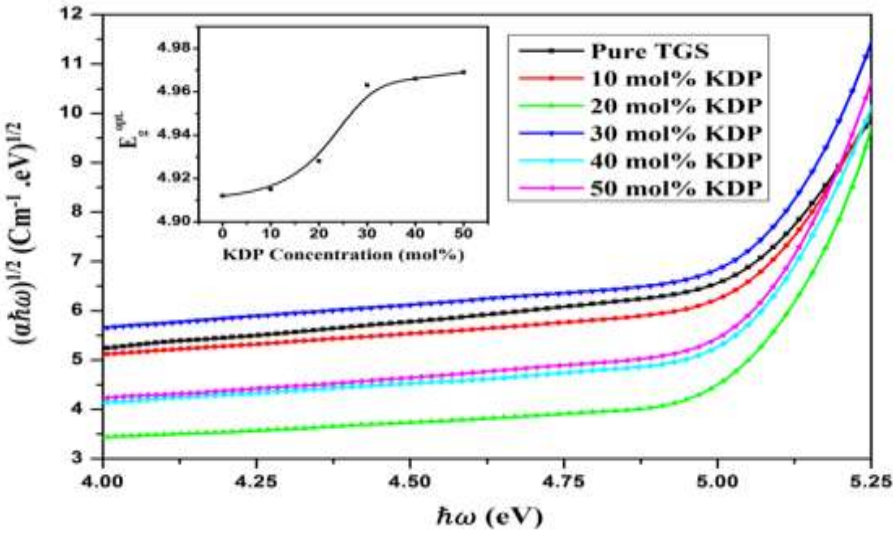

Fig. 2. Plot of $(\alpha\hbar\omega)^{1/2}$ verses $\hbar\omega$ for KDPTGS single crystals (inset plot of indirect optical energy gap $E_g^{opt.}$ against KDP concentration).

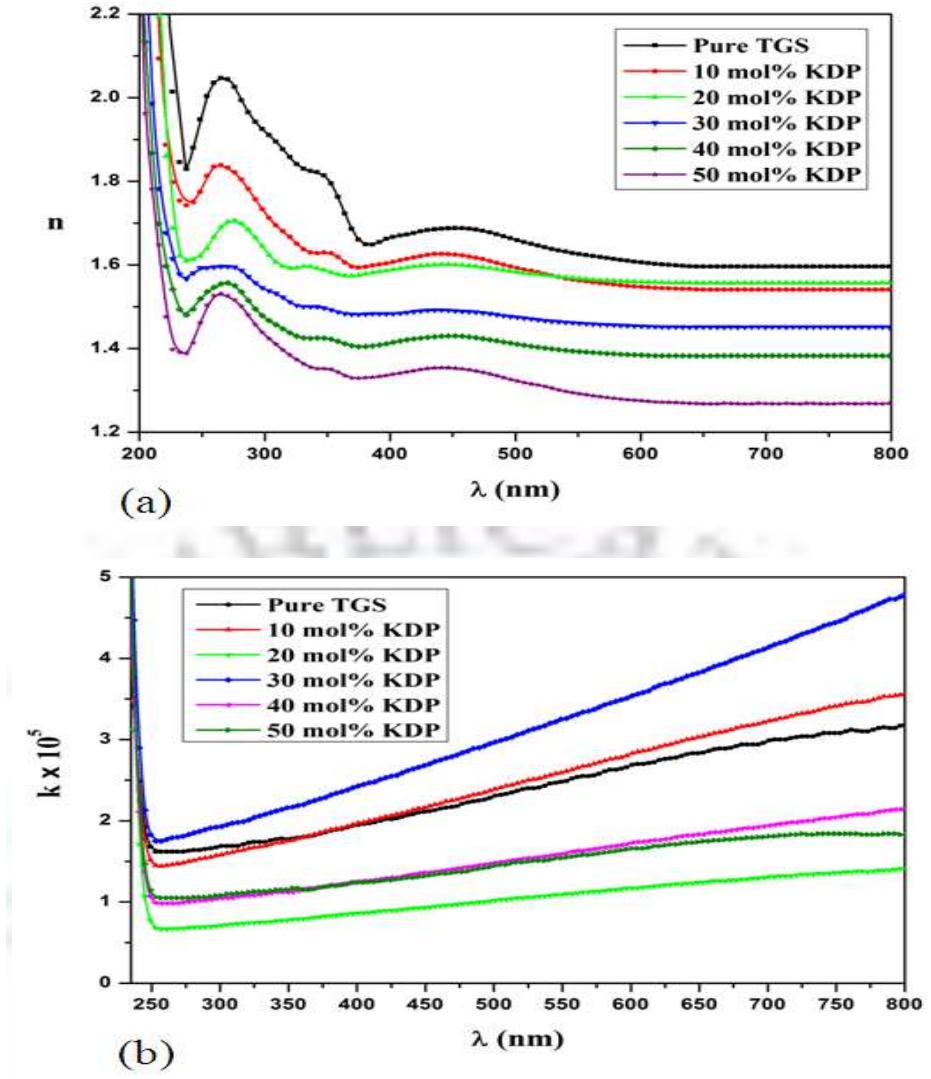

Fig. 3. Spectral behavior of (a) refractive index n and (b) extension coefficient k for KDPTGS single crystals.

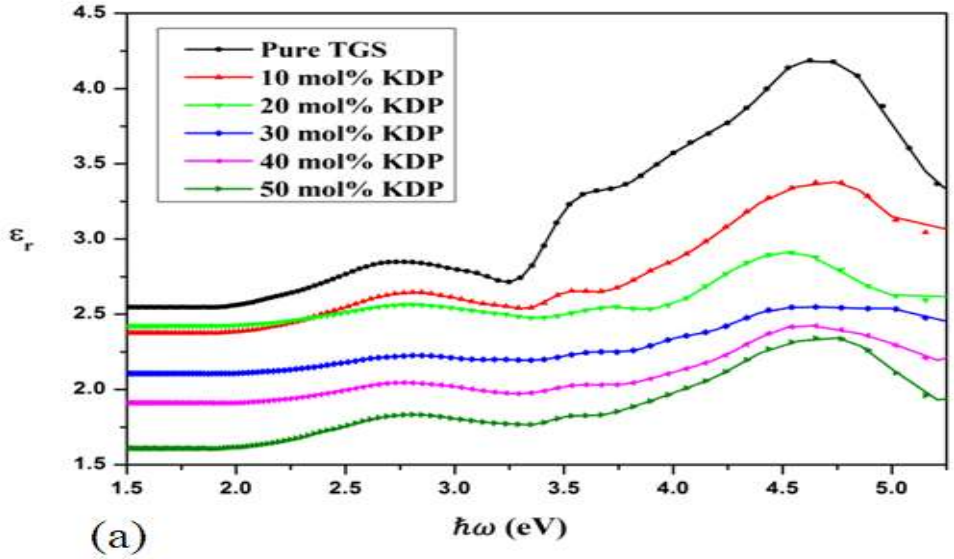

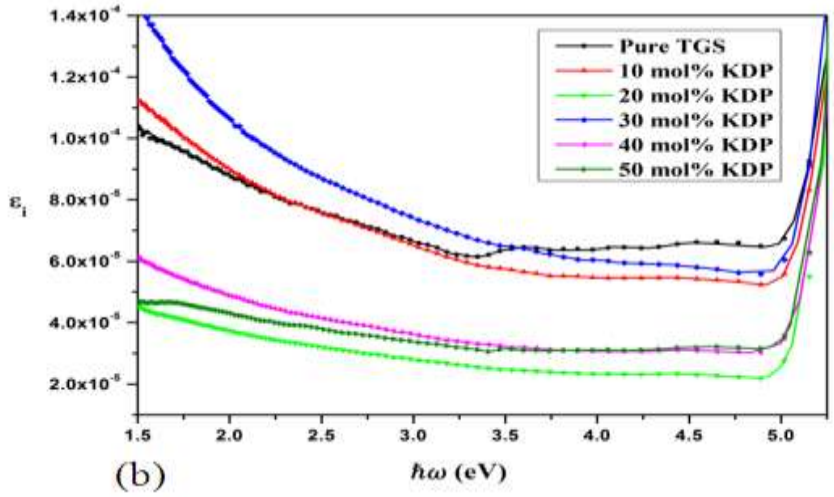

Fig. 4. Variation of the (a) real ε_r and (b) imaginary ε_i parts of the dielectric constant for KDPTGS single crystals.

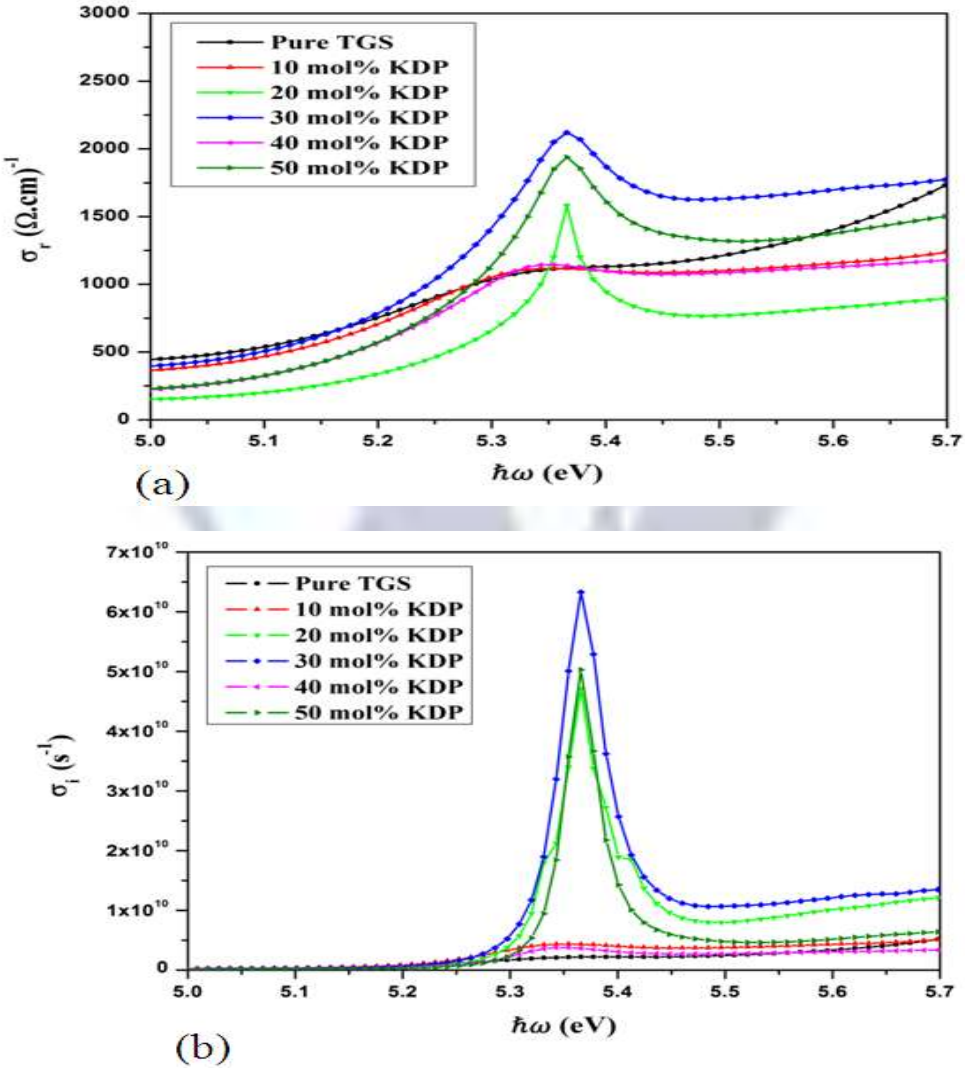

Fig. 5. Spectra of the (a) real σ_r and (b) imaginary σ_i parts of the optical conductivity of KDPTGS single crystals.

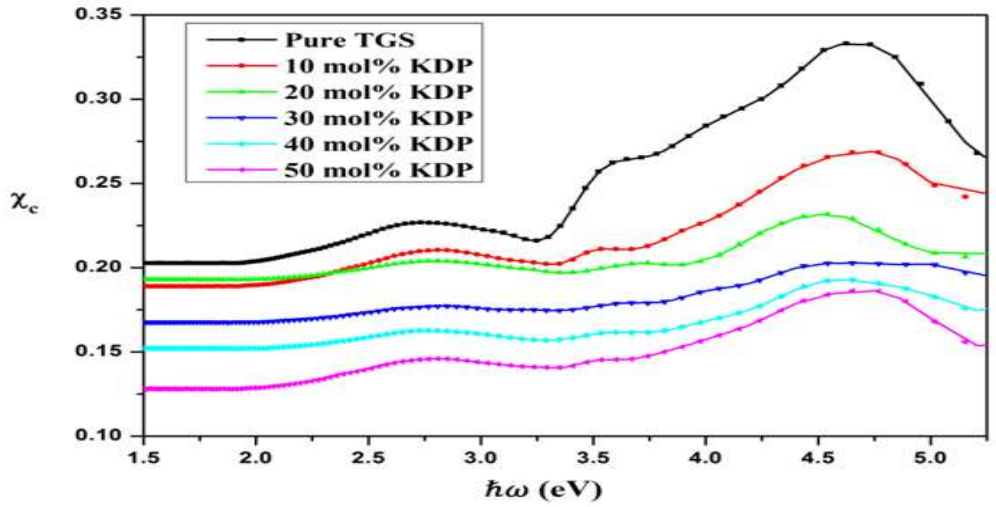

Fig. 6. Relation between electric susceptibility χ_c as a function of photon energy $\hbar\omega$ for KDPTGS single crystals.

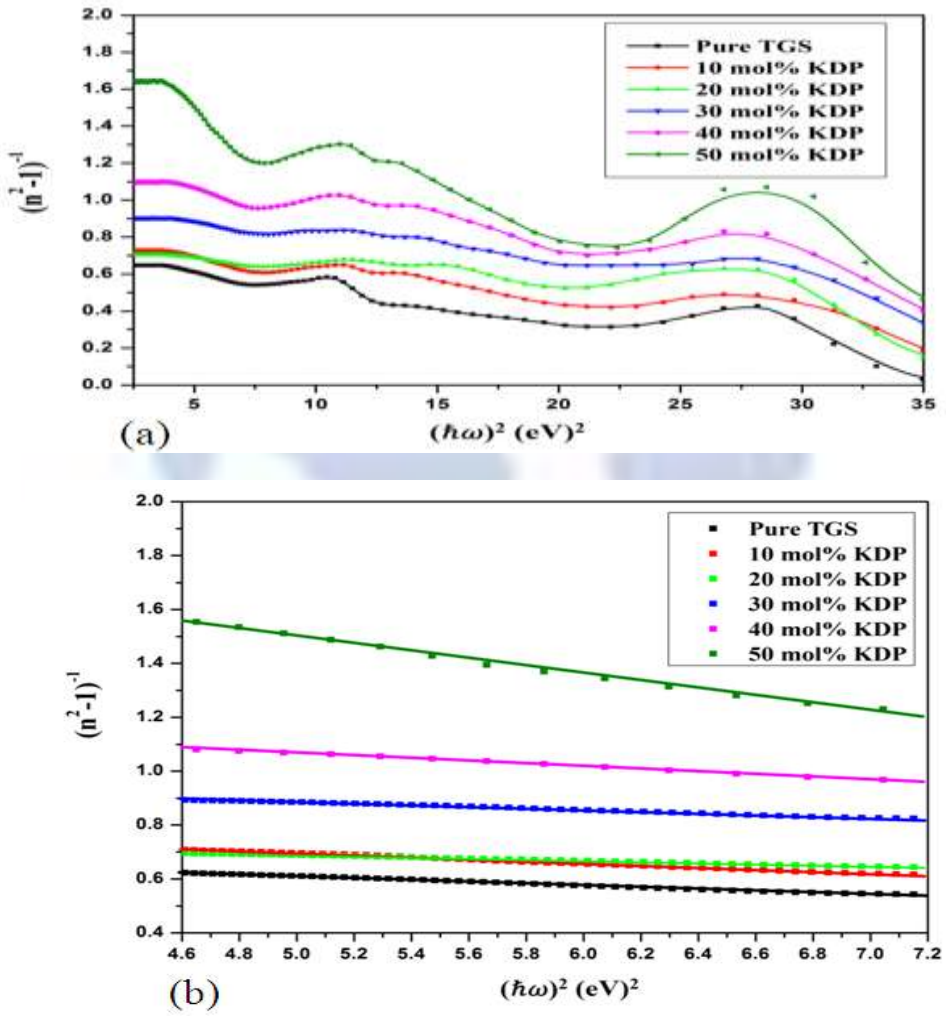

Fig. 7. (a) The relation between $(n^2-1)^{-1}$ and the squared photon energy $(\hbar\omega)^2$ for KDPTGS single crystals. (b) $(n^2-1)^{-1}$ and $(\hbar\omega)^2$ fitted to the best straight line in the photon energy range ($\hbar\omega$ = 4.6 - 7.2eV).

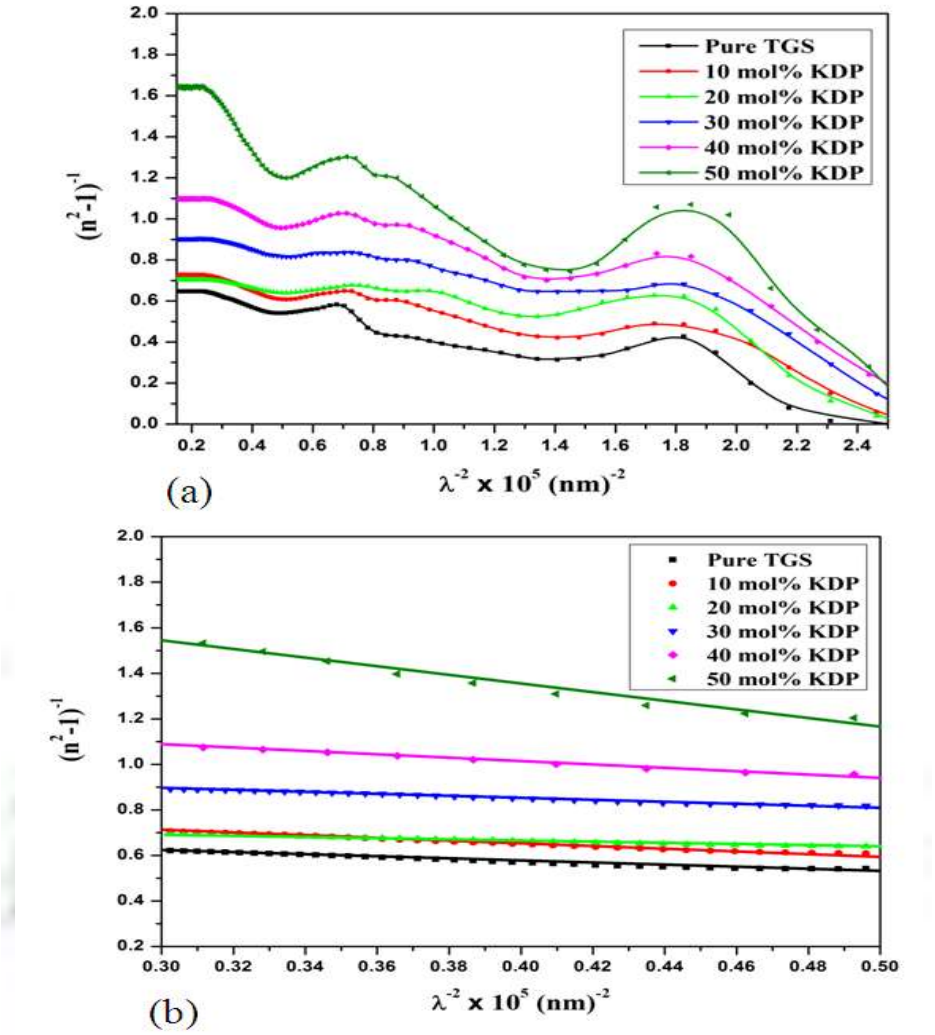

Fig. 8.(a) : Variation of $(n^2-1)^{-1}$ verses λ^{-2}(b) $(n^2-1)^{-1}$verses λ^{-2} fitted to the best straight line in the range (0.2−2.4) x$10^5$$(nm)^{-2}$.

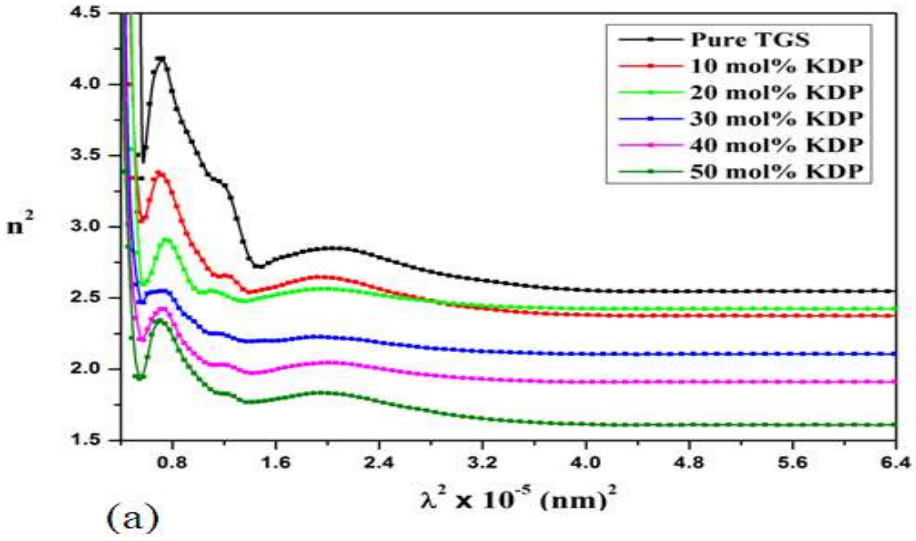

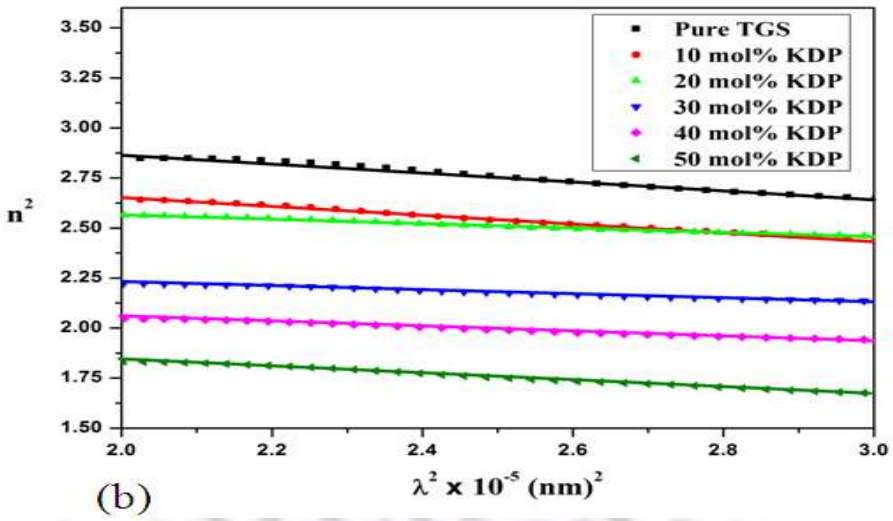

Fig. 9. (a) The relation between n^2 and λ^2 (b)n^2 and λ^2 fitted to the best straight linein the range (2−3) x10^{-5}(nm)^2.